

Stronger Hardy's quantum nonlocality: theory and simulation

Duc Minh Tran,¹ Van-Duy Nguyen,² Le Bin Ho,^{3,4} and Hung Q. Nguyen^{1,*}

¹*Nano and Energy Center, University of Science,
Vietnam National University, Hanoi, 120401, Vietnam*

²*Phenikaa Institute for Advanced Study, Phenikaa University, Hanoi 12116, Vietnam*

³*Frontier Research Institute for Interdisciplinary Sciences, Tohoku University, Sendai 980-8578, Japan*

⁴*Department of Applied Physics, Graduate School of Engineering, Tohoku University, Sendai 980-8579, Japan*

Depending on the way one measures, quantum nonlocality might manifest more visibly. Using basis transformations and interactions on a particle pair, Hardy logically argued that any local hidden variable theory leads to a paradox. Extended from the original work, we introduce a quantum nonlocal scheme for n -particles ensembles using two distinct approaches. First, a theoretical model is derived with analytical results for nonlocal conditions and probability. Second, a quantum simulation using quantum circuits is constructed that matches very well to the analytical theory. Executing this experiment on real quantum computers for $n = 3$, we obtain reasonable results compared to theory. As n grows, the nonlocal probability asymptotes 15.6%, implying that nonlocality might persist even at macroscopic scales.

Introduction.— Through gedanken experiment on particle-antiparticle interactions inside two intertwined Mach-Zehnder interferometers, Hardy delivered a contextuality of nonlocal quantum mechanics without using inequalities [1, 2], an all-versus-nothing criterion for *local hidden variable* (LHV) theory. Due to the nonlocal nature of quantum states, it is possible to argue the pair met without an annihilation event, causing a paradox. Suppose we have two physical observables $U_i = |u_i\rangle\langle u_i|$ and $D_i = |d_i\rangle\langle d_i|$ with their basis transformation

$$\begin{aligned} |u_i\rangle &= A^*|c_i\rangle - B|d_i\rangle, & |v_i\rangle &= B^*|c_i\rangle + A|d_i\rangle, \\ |c_k\rangle &= A|u_k\rangle + B|v_k\rangle, & |d_k\rangle &= -B^*|u_k\rangle + A^*|v_k\rangle, \end{aligned}$$

where $|A|^2 + |B|^2 = 1$. With N being the normalization factor, the quantum state writes in equivalent forms:

$$|\Psi\rangle = N(|c_1\rangle|c_2\rangle - A^2|u_1\rangle|u_2\rangle) \quad (1)$$

$$= N(AB|u_1\rangle|v_2\rangle + AB|v_1\rangle|u_2\rangle + B^2|v_1\rangle|v_2\rangle) \quad (2)$$

$$= N(|c_1\rangle(A|u_2\rangle + B|v_2\rangle) - A^2(A^*|c_1\rangle - B|d_1\rangle)|u_2\rangle) \quad (3)$$

$$= N((A|u_1\rangle + B|v_1\rangle)|c_2\rangle - A^2|u_1\rangle(A^*|c_2\rangle - B|d_2\rangle)) \quad (4)$$

$$= N(|c_1\rangle|c_2\rangle - A^2(A^*|c_1\rangle - B|d_1\rangle)(A^*|c_2\rangle - B|d_2\rangle)). \quad (5)$$

Hardy's original argument can be divided into three set of nonlocal conditions. Firstly in (1) and (2), the two particles start as a separable state $|c_1\rangle|c_2\rangle$, but are entangled by an interaction which effectively quench the $|u_1\rangle|u_2\rangle$ substate when measuring $|\Psi\rangle$ in $\{|u_i\rangle, |v_i\rangle\}$ basis. In other words, the probability to find $U_1 = 1$ and $U_2 = 1$ simultaneously is zero: $P(U_1U_2) = 0$. Here and throughout the paper, we write $P(U_1U_2 \dots) = 0$ as a shorthand for $P(U_1U_2 \dots = 1) = 0$. Secondly in (3) and (4), LHV-correlations between U_i and D_i are established by mixing measurement basis for different particles. Using conventional notations for conditional probability, the

probability that $U_2 = 1$ under the condition of $D_1 = 1$ is $P(U_2|D_1) = 1$. Similarly, $P(U_1|D_2) = 1$. Finally in (5), $P(D_1D_2) > 0$, when combined with the secondly established probabilities would imply $P(U_1U_2) > 0$. This last nonzero probability directly contradicts the first nonlocal condition, which is $P(U_1U_2) = 0$.

This elegant approach was quickly extended to many aspects of 2-particle states [3–9], 3-particle states [10–12], or arbitrary n -particle states [13–17]. It is found that Hardy-type nonlocality proof can be formed from GHZ states [11, 16, 17], graph states [18, 19], symmetric states [20], W and Dicke states [21], and Wigner's argument [22]. Its strength and visibility compared to other nonlocality proof such as Bell's theorem, GHZ and CHSH are explored [23–26], and there are several attempts at unification [27, 28]. The nonlocal visibility can also be amplified using “ladder” logic [29–31], graph-theoretic logic [32, 33], and high-dimensional systems [34–37]. Meanwhile, the correlation between nonlocality and entanglement is at the spotlight in quantum foundation [4, 38–43]. More importantly, there are experimental evidences in photons [44–48], atoms [49–52], superconducting circuits [53, 54], and generic quantum computers [55, 56].

To derive a Hardy's type paradox, one starts with choosing a specific quantum state, such as GHZ or W . After establishing a set of nonlocal conditions for the chosen state, the nonlocal probability is calculated verifying these assumptions. In this work, we follow this strategy and find a particular version of Hardy's paradox that yields a very high nonlocal probability that approaches 15.6% as the ensemble size n grows. Besides the theoretical description, we provide a quantum simulation by using quantum circuits on any simulators and any available quantum hardware. We perform this experiment on IBM quantum computers and obtain data that match reasonable well to theory.

n-particle Hardy's paradox— Consider an ensemble of n qubits labeled by $\Omega = \{1, \dots, n\}$. For each qubit

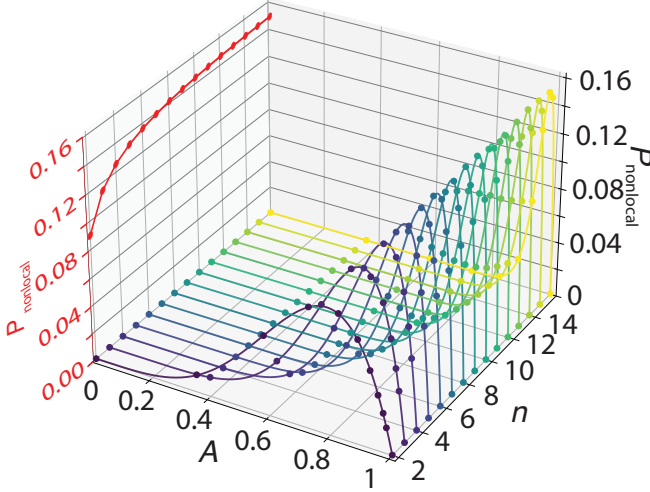


FIG. 1. **Analytical result:** Nonlocal probability P_{nonlocal} as a function of the transformation coefficient A at different ensemble size n . The red curve on the left is a projection of the maximum P_{nonlocal} for different n . Solid lines are analytical result Eq. (18), while dots are simulation result obtained from the QASM quantum simulator provided by IBM.

$k \in \Omega$ in its local realistic space, we introduce two non-commuting pair of observables $U_k = |u_k\rangle\langle u_k|$, $V_k = |v_k\rangle\langle v_k|$ and $C_k = |c_k\rangle\langle c_k|$, $D_k = |d_k\rangle\langle d_k|$ that span two orthogonal bases $\{|u_k\rangle, |v_k\rangle\}$ and $\{|c_k\rangle, |d_k\rangle\}$. The two bases obey a general set of relations

$$|u_k\rangle = A_k^*|c_k\rangle - B_k|d_k\rangle, \quad |v_k\rangle = B_k^*|c_k\rangle + A_k|d_k\rangle, \quad (6)$$

$$|c_k\rangle = A_k|u_k\rangle + B_k|v_k\rangle, \quad |d_k\rangle = -B_k^*|u_k\rangle + A_k^*|v_k\rangle, \quad (7)$$

where A_k, B_k are complex coefficients satisfying $|A_k|^2 + |B_k|^2 = 1$. Following notations in Ref. [17], we denote $\mathcal{U}_\alpha \equiv \Pi_{k \in \alpha} U_k$ and $\mathcal{D}_\alpha \equiv \Pi_{k \in \alpha} D_k$ for any subset $\alpha \subseteq \Omega$, and likewise $\mathcal{A}_\alpha \equiv \Pi_{k \in \alpha} A_k$ and $\mathcal{B}_\alpha \equiv \Pi_{k \in \alpha} B_k$. In our indices, Latin letters denote numbers and Greek letters denote sets of number. For an arbitrary set α , let $|\alpha|$ be its cardinality - i.e. the number of elements in α , $\mathcal{P}(\alpha)$ be its power set, and $\bar{\alpha} = \{\Omega \setminus \alpha\}$. The state of interest is a general n -particle state in the $\{|u_k\rangle, |v_k\rangle\}^{\otimes n}$ basis *without* the $|u_1\rangle \otimes |u_2\rangle \otimes \dots \otimes |u_n\rangle \equiv |u_1 u_2 \dots u_n\rangle$ term:

$$|\Psi_n\rangle = N[|c_1 c_2 \dots c_n\rangle - \mathcal{A}_\Omega|u_1 u_2 \dots u_n\rangle] \quad (8)$$

$$= N[\mathcal{A}_{\Omega \setminus \{n\}} B_n |u_1 u_2 \dots v_n\rangle + \dots + \mathcal{B}_{\Omega} |v_1 v_2 \dots v_n\rangle] \quad (9)$$

$$= N \sum_{\alpha \subseteq \mathcal{P}(\Omega) \setminus \{\Omega\}} \mathcal{A}_\alpha \mathcal{B}_{\bar{\alpha}} \bigotimes_{i \in \alpha} |u_i\rangle \otimes \bigotimes_{j \in \bar{\alpha}} |v_j\rangle. \quad (10)$$

The tensor product is ordered by Latin indices with normalization constant $N = [1 - |\mathcal{A}_\Omega|^2]^{-1/2}$ [57]. Then, measuring $|\Psi_n\rangle$ in $\{|u_k\rangle, |v_k\rangle\}^{\otimes n}$ yields the first nonlocal condition

$$P(\mathcal{U}_\Omega) \equiv P(U_1 U_2 \dots U_n) = 0, \quad (11)$$

for the term without $|u_1 u_2 \dots u_n\rangle$.

For the next n conditions, $|\Psi_n\rangle$ is examined in mixed bases. Measuring particle $k^{\text{th}} \in \Omega$ in $\{|c_k\rangle, |d_k\rangle\}$ while others are in $\{|u\rangle, |v\rangle\}$, we have

$$|\Psi_n\rangle = N \left[|B_k|^2 \mathcal{A}_{\bar{\kappa}} |u_1 \dots u_{k-1} c_k u_{k+1} \dots u_n\rangle \right. \\ \left. + \sum_{\alpha \in \mathcal{P}(\bar{\kappa}) \setminus \{\bar{\kappa}\}} \mathcal{A}_\alpha \mathcal{B}_{\bar{\kappa} \setminus \alpha} \bigotimes_{i \in \alpha} |u_i\rangle \otimes \bigotimes_{j \in \bar{\kappa} \setminus \alpha} |v_j\rangle \otimes |c_k\rangle \right. \\ \left. + B_k \mathcal{A}_\Omega |u_1 \dots u_{k-1} d_k u_{k+1} \dots u_n\rangle \right]. \quad (12)$$

Here, $\kappa = \{k\}$, then $\bar{\kappa} = \Omega \setminus \kappa$. The second set of n nonlocal conditions writes as conditional probabilities

$$P(\mathcal{U}_{\bar{\kappa}} | D_k) = 1, \quad \forall k \in \Omega, \quad (13)$$

which establishes an LHV-correlation that $D_k = 1 \Rightarrow \mathcal{U}_{\bar{\kappa}} \equiv U_1 U_2 \dots U_{k-1} U_{k+1} \dots U_n = 1$. Every time we measure $|\Psi\rangle$, if $D_k = 1$ then $\mathcal{U}_{\bar{\kappa}} = 1$, or $P(D_k) \leq P(\mathcal{U}_{\bar{\kappa}})$. Hence, if 2 particles simultaneously yield $D_k D_l = 1$, $l \neq k$, then $\mathcal{U}_\Omega \equiv U_1 U_2 \dots U_n = 1$. With $\bar{\lambda} = \Omega \setminus \{l\}$, the second set of conditions Eq. (13) also writes

$$P(D_k D_l) < P(\mathcal{U}_{\bar{\kappa} \cup \bar{\lambda}}) = P(\mathcal{U}_\Omega), \quad \forall k, l \in \Omega, l \neq k. \quad (14)$$

Therefore, measuring $|\Psi_n\rangle$ should not yield $D_k D_l = 1$, $l \neq k$. However, the third set of conditions writes

$$P(\mathcal{D}_\alpha) > 0, \quad \forall \alpha \in \mathcal{P}(\Omega), |\alpha| \geq 2, \quad (15)$$

which we call the nonlocal probabilities, resulting in $P(\mathcal{U}_\Omega) > 0$, which contradicts Eq. (11). We emphasize that there are more than one condition in Eq. (15).

In $\{|c_k\rangle, |d_k\rangle\}^{\otimes n}$ basis, $|\Psi_n\rangle$ from Eq. (8) is rewritten

$$|\Psi_n\rangle = N \left[|c_1 \dots c_n\rangle - \mathcal{A}_\Omega (A_k^*|c_k\rangle - B_k|d_k\rangle)^{\otimes n} \right]. \quad (16)$$

There are many substates containing two or more qubits with $| \dots d_k \dots d_l \dots \rangle$. They all satisfy Eq.(15). From the binomial theorem, there are $\sum_{k=2}^n \binom{n}{k} = 2^n - n - 1$ of them, constituting a combined nonlocal probability of

$$P_{\text{nonlocal}} = |\mathcal{A}_\Omega|^2 - \frac{|\mathcal{A}_\Omega|^4}{1 - |\mathcal{A}_\Omega|^2} \sum_{k=1}^n \frac{1 - |A_k|^2}{|A_k|^2}. \quad (17)$$

It reaches the maximum when all $|A_k|$ equals, $|A_k| = A \quad \forall k \in \Omega$. For this reason we only consider A real in our data. Eq. (17) becomes

$$P_{\text{nonlocal}} = A^{2n} - n \frac{A^{4n-2}(1 - A^2)}{1 - A^{2n}}. \quad (18)$$

All calculation to obtain these results is provided in detail in the supplementary material [57].

These results are displayed in Fig. 1. P_{nonlocal} as smooth curves for different ensemble size n are plotted as a function of A . In Hardy's original setup, A controls

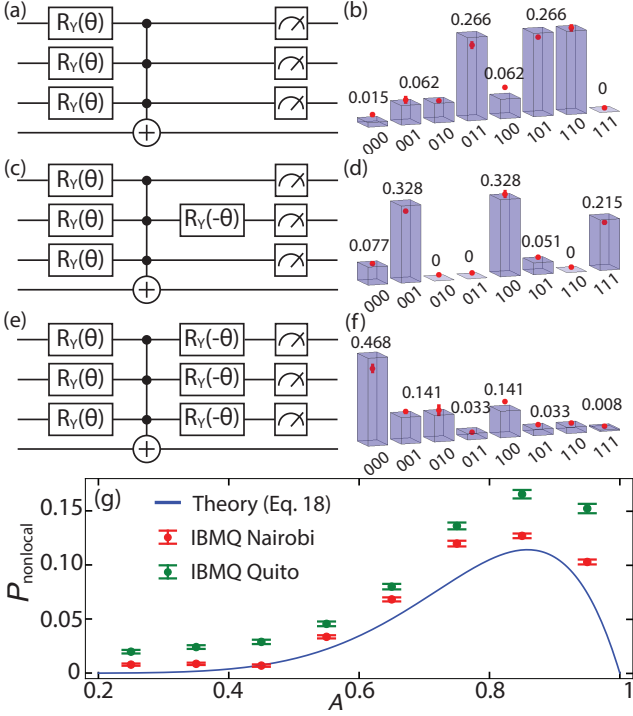


FIG. 2. Quantum simulation: Quantum circuits for $n = 3$ and their results executed at $A = 0.9$, corresponding to a rotation of $\theta = 0.713\pi$. Numbers and bars on the histogram are theoretical probabilities obtained from a quantum simulator, and red dots are experimental result from IBM's Nairobi. (a, b) The first set of nonlocal condition. A quantum state $|\Psi_3\rangle$ is prepared without $|u_1u_2u_3\rangle$, evidently from $|111\rangle$'s probability in (b). (c, d) The second set of nonlocal conditions. Rotating the second qubit back to $\{|c_2\rangle, |d_2\rangle\}$ while leaving other qubits in $\{|u\rangle, |v\rangle\}$. $D_2 = 1 \Rightarrow U_1U_3 = 1$. (e, f) The last nonlocal conditions: applying $R_Y(-\theta)$ on all qubits. The probability for $D_kD_l = 1, l \neq k$ is nonzero, thus establishing a Hardy-type paradox. (g) Experimental results obtained from IBM's transmon processor Quito in green and Nairobi in red, averaging from 100 executions each with 20000 shots.

the transmission coefficients of the beamsplitters. The red curve projects P_{nonlocal} maximal value for each n . It indicates that P_{nonlocal} asymptotes 15.6% as n grows. Dots are results from a quantum simulation that runs on a virtual machine, as presented in the following section.

Quantum simulation— The above analysis can be realized on quantum hardware. Here, we implement these results to measure the nonlocality of the quantum state $|\Psi_n\rangle$ on a quantum circuit. Figure 2 illustrates our approach for $|\Psi_3\rangle$, i.e. $n = 3$. The left column contains three quantum circuits that are consistent with the sets of nonlocal conditions Eq. (11), (13), (15). The right column shows their result for specific value $A = 0.9$. Rotation gates $R_Y(\theta)$ transform each of them from XY plane to XZ plane, corresponding to a basis transformation from $\{|c\rangle, |d\rangle\}$ to $\{|u\rangle, |v\rangle\}$ basis. The transformation

coefficient A , therefore, relates to θ as $A_k = \sin(\theta_k/2)$. State $|\Psi_n\rangle$ is constructed using post-selection scheme [45, 46, 58] with the help of a Toffoli gate targeting an auxiliary qubit. It is straightforward to generalize this quantum circuit to the case of an arbitrary n . In this case, the Toffoli gate is instead controlled by all n qubits.

The first condition Eq. (11) is satisfied by a state preparation with “zero-probability substates” in it that excludes $|u_k\rangle^{\otimes n}$. We begin with $|\Psi_{\text{start}}\rangle = |c_k\rangle^{\otimes n}$, then a set of rotation gates $R_Y(\theta_k)$ transforms $|\Psi_{\text{start}}\rangle$ into $\{|u_k\rangle, |v_k\rangle\}^{\otimes n}$ basis. The Toffoli gate marks $|u_k\rangle^{\otimes n}$ to help post-selecting $|\Psi_n\rangle$, following Eq. (11). For $n = 3$, the circuit in Fig. 2a satisfies the first set of nonlocal conditions and yields $\langle u_1u_2u_3|\Psi_3\rangle = 0$, which is confirmed in Fig. 2b with $P(111) = 0$.

The second set of conditions Eq. (13) is tested by measuring the k^{th} qubit in $\{|c_k\rangle, |d_k\rangle\}$ basis, while leaving others in their $\{|u_k\rangle, |v_k\rangle\}$ bases. This is done on the circuit by applying a single $R_Y(-\theta_k)$ on the k^{th} qubit. In Fig. 2c, if the measurement yields $D_2 = 1$, it ensures $U_1 = U_3 = 1$. This means $P(U_1D_2U_3) \equiv P(111) = 0.215 > 0$, while $P(V_1D_2U_3) \equiv P(011) = 0$, $P(U_1D_2V_3) \equiv P(110) = 0$, and $P(V_1D_2V_3) \equiv P(010) = 0$, as shown in Fig. 2d. It is straightforward to verify that $R_Y(-\theta_k)$ has a similar effect when applied on $|q_1\rangle$ or $|q_3\rangle$, or the case of generalized n . In other words, the same correlation is found when measuring $D_1U_2U_3$ or $U_1U_2D_3$.

The third set of conditions Eq. (15) is a nonzero total probability of measurements that contradicts previous conditions, generally tested in $\{|c_k\rangle, |d_k\rangle\}^{\otimes n}$. To check, we apply $R_Y(-\theta_k)$ on all qubits and measure them in $\{|c_k\rangle, |d_k\rangle\}^{\otimes n}$ basis. For $n=3$, these states are $|d_1d_2c_3\rangle$, $|d_1c_2d_3\rangle$, $|c_1d_2d_3\rangle$, and $|d_1d_2d_3\rangle$. In our quantum circuit, the corresponding states are $|110\rangle$, $|101\rangle$, $|011\rangle$, and $|111\rangle$, which yield a combined probability of 0.107 as shown in Fig. 2f, in agreement with theoretical result in Eq. (18) for $A = 0.9$ and $n = 3$. Henceforth, all nonlocal conditions are satisfied, and a Hardy-type paradox is established.

Obtaining identical result for P_{nonlocal} , but our analytical calculation and the quantum simulation are different approaches. While the first part is a theoretical model of nonlocality, the second part is an experimental protocol to probe nonlocality that can be implemented on real quantum hardware. For example, realizing the circuit on an optical quantum computer would produce n intertwined Mach-Zehnder interferometers. To demonstrate its practical aspect, we execute the quantum circuit in Fig. 2e on IBM's quantum computers Nairobi and Quito [59] and obtain results shown on Fig. 2g, averaging from 2 million shots each, equally divided into 100 different runs. Apparently, the systematic errors on Quito are slightly larger than those on Nairobi. These are the best results we obtain from IBM's transmon processors. Any experiment for $n > 3$ yields result with big error, as compared to IBM's own QASM simulator.

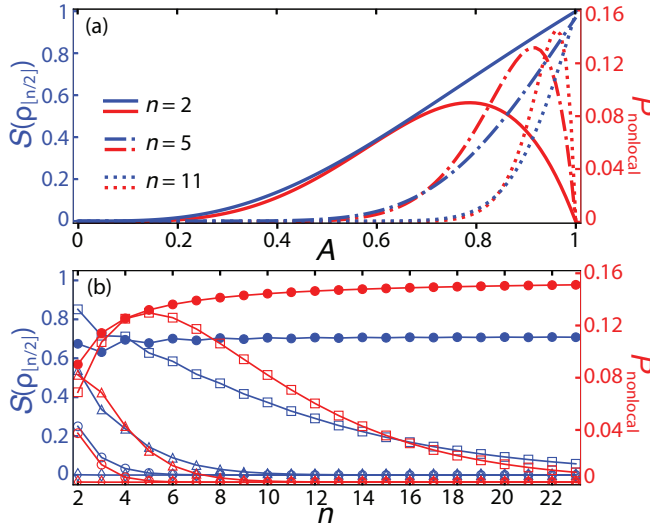


FIG. 3. **Entanglement entropy:** von Neumann entropy $S(\rho_{[n/2]})$ calculated at half-chain bipartition is shown on the left axis in blue. In direct comparison, P_{nonlocal} per Eq. (18) is shown on the right axis in red. (a) $S(\rho_{[n/2]})$ and P_{nonlocal} as a function of the transformation coefficient A at $n = 2, 5$, and 11 . (b) $S(\rho_{[n/2]})$ and P_{nonlocal} as a function of n at $A = 0.1$ (open diamonds), 0.5 (open circles), 0.7 (open triangles), and 0.9 (open squares). The solid circles are data obtained at the optimum A , i.e. at the maximum of P_{nonlocal} .

Nonlocality and entanglement— The connection between entanglement and quantum nonlocality is one of contentious nature [39–42]. To further study $|\Psi_n\rangle$, its entanglement is calculated under half-chain bipartition using von Neumann entropy. Let $\rho = |\Psi_n\rangle\langle\Psi_n|$ be the density matrix of $|\Psi_n\rangle$ on the Hilbert space $\mathcal{H} = \mathcal{H}_A \otimes \mathcal{H}_B$. Then, \mathcal{A} 's reduced density matrix is $\rho_{\mathcal{A}} = \text{tr}_{\mathcal{B}}(\rho)$. The von Neumann entropy at half-chain bipartition writes

$$S(\rho_{[n/2]}) = -\text{tr}(\rho_{[n/2]} \log_2 \rho_{[n/2]}), \quad (19)$$

with $\lfloor n/2 \rfloor$ denotes the floor of $n/2$. These two quantities P_{nonlocal} and $S(\rho_{[n/2]})$ are compared in Fig. 3 as a function of the transformation coefficient A and the size n . Apparently, their behavior are completely different. While P_{nonlocal} increases to a maximum and then decreases sharply, $S(\rho_{[n/2]})$ grows monotonically. It implies that high entanglement does not always correlate to high nonlocality [39, 40, 42]. Another trend is observed when $S(\rho_{[n/2]})$ and P_{nonlocal} are plotted as a function of n for different A , shown in Fig. 3b. Only for optimal A , P_{nonlocal} and $S(\rho_{[n/2]})$ approach a constant as n grows, as shown by solid circles in Fig. 3b. Parallel analyses under a different bipartition for one- versus-the-rest of the system, and using the positive partial transpose (PPT), also show monotonic increases [57].

Discussion and Conclusion— Apparently, $|\Psi_n\rangle$ defined in Eq. (8) is not a common state such as GHZ, W, or Dicke. Indeed, our choice was inspired by the

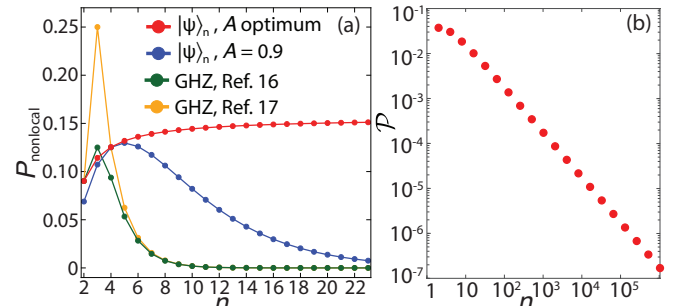


FIG. 4. **Nonlocality at the macroscopic scale:** (a) P_{nonlocal} for $|\Psi_n\rangle$ per Eq. (18) at two values: $A = 0.9$ and A optimum are directly compared to results for generalized GHZ state in Eq. (28), Ref. [16] and Eq. (2), Ref. [17]. (b) The total nonlocal probability \mathcal{P} quickly reduces to zero as n grows in a log-log plot.

symmetry in the quantum circuit that simulates original Hardy's paradox in our previous work [60]. Here, the generalized quantum circuit is a natural extension from Fig. 4b in Ref. [60] where the Toffoli gate is controlled by all n qubits.

As n grows, P_{nonlocal} quickly reduces to zero at fixed A , as shown in Fig. 4a for a representative value $A = 0.9$. This observation matches with previous work on generalized GHZ states. At $n = 2$, $P_{\text{nonlocal}} = 9\%$ because they are all equal to the original Hardy's result. The fast reduction of P_{nonlocal} at large n in Ref. [16, 17] might relates to the nature of GHZ states. Although maximally entangled, GHZ states do not necessarily reach maximum in nonlocality [39–42]. There is an optimum value of $A = |A_k| \forall k \in \Omega$ that P_{nonlocal} is maximized whereas the entanglement entropy $S(\rho_{[n/2]})$ behaves monotonically.

However, it is difficult to detect this nonlocal probability of 15.6% at the macroscopic scale. The total nonlocal probability of an n -ensemble can be calculated from the area of the $P_{\text{nonlocal}}(A)$ curve $\mathcal{P} = \int_0^1 P_{\text{nonlocal}}(A) dA$. As seen in Fig. 4b, \mathcal{P} quickly reduces to zero as n grows. This is also evident from Fig. 1, as the probability curves become narrower with larger n . A small change in the transformation coefficient A leads to a large drop in P_{nonlocal} . Still, interestingly, there is a high chance nonlocality persists even at macroscopic scales.

In summary, we have extended the original Hardy's paradox to a general case and obtained a nonlocality with probability approaching 15.6% as the ensemble size grows. The nonlocal conditions and nonlocal probability are derived analytically. A quantum simulation is proposed that matches well to the theory, especially when tested on real quantum computers.

Acknowledgement— HQN would like to thank Dr. Nguyen Hoang Hai and Dr. Nguyen The Toan for helpful discussions.

* hungngq@hus.edu.vn

[1] L. Hardy, Physical Review Letters **68**, 2981–2984 (1992).

[2] L. Hardy, Physical Review Letters **71**, 1665–1668 (1993).

[3] S. Popescu and D. Rohrlich, Physics Letters A **166**, 293 (1992).

[4] S. Goldstein, Physical Review Letters **72**, 1951–1951 (1994).

[5] A. Cabello, Phys. Rev. A **61**, 022119 (2000).

[6] M. Żukowski, i. c. v. Brukner, W. Laskowski, and M. Wieśniak, Phys. Rev. Lett. **88**, 210402 (2002).

[7] M. Yang, H.-X. Meng, J. Zhou, Z.-P. Xu, Y. Xiao, K. Sun, J.-L. Chen, J.-S. Xu, C.-F. Li, and G.-C. Guo, Phys. Rev. A **99**, 032103 (2019).

[8] G. Vallone, I. Gianani, E. B. Inostroza, C. Saavedra, G. Lima, A. Cabello, and P. Mataloni, Phys. Rev. A **83**, 042105 (2011).

[9] T. F. Jordan, Phys. Rev. A **50**, 62 (1994).

[10] X. hua Wu and R. hua Xie, Physics Letters A **211**, 129 (1996).

[11] X.-H. Wu, H.-S. Zong, and H.-R. Pang, Physics Letters A **276**, 221 (2000).

[12] S. Ghosh, G. Kar, and D. Sarkar, Physics Letters A **243**, 249 (1998).

[13] G. Kar, Physical Review A **56**, 1023–1024 (1997).

[14] S. Ghosh and S. M. Roy, Journal of mathematical physics **51**, 122204 (2010).

[15] C. Pagonis and R. Clifton, Physics Letters A **168**, 100 (1992).

[16] J. L. Cereceda, Physics Letters A **327**, 433–437 (2004).

[17] S.-H. Jiang, Z.-P. Xu, H.-Y. Su, A. K. Pati, and J.-L. Chen, Physical Review Letters **120**, 10.1103/physrevlett.120.050403 (2018).

[18] A. Cabello, O. Gühne, P. Moreno, and D. Rodríguez, Laser Physics **18**, 335 (2008).

[19] M. Gachechiladze, C. Budroni, and O. Gühne, Phys. Rev. Lett. **116**, 070401 (2016).

[20] Z. Wang and D. Markham, Phys. Rev. Lett. **108**, 210407 (2012).

[21] T. J. Barnea, G. Pütz, J. B. Brask, N. Brunner, N. Gisin, and Y.-C. Liang, Phys. Rev. A **91**, 032108 (2015).

[22] D. Home, D. Saha, and S. Das, Phys. Rev. A **91**, 012102 (2015).

[23] A. Garuccio, Phys. Rev. A **52**, 2535 (1995).

[24] W. van Dam, P. Grunwald, and R. Gill, IEEE Transactions on Information Theory **51**, 2812 (2005).

[25] G. Ghirardi and L. Marinatto, Physics Letters A **372**, 1982 (2008).

[26] D. Braun and M.-S. Choi, Phys. Rev. A **78**, 032114 (2008).

[27] L. Mančinska and S. Wehner, Journal of Physics A: Mathematical and Theoretical **47**, 424027 (2014).

[28] Z. Dong, Y. Yang, and H. Cao, International Journal of Theoretical Physics **59**, 1644 (2020).

[29] D. Boschi, S. Branca, F. De Martini, and L. Hardy, Phys. Rev. Lett. **79**, 2755 (1997).

[30] M. Barbieri, F. De Martini, G. Di Nepi, and P. Mataloni, Physics Letters A **334**, 23 (2005).

[31] A. Cabello, P. Badziag, M. Terra Cunha, and M. Bourennane, Phys. Rev. Lett. **111**, 180404 (2013).

[32] A. Sohbi and J. Kim, Phys. Rev. A **100**, 022117 (2019).

[33] K. Svozil, Phys. Rev. A **103**, 022204 (2021).

[34] J.-L. Chen, A. Cabello, Z.-P. Xu, H.-Y. Su, C. Wu, and L. C. Kwek, Physical Review A **88**, 10.1103/physreva.88.062116 (2013).

[35] L. Chen, W. Zhang, Z. Wu, J. Wang, R. Fickler, and E. Karimi, Phys. Rev. A **96**, 022115 (2017).

[36] H.-X. Meng, J. Zhou, Z.-P. Xu, H.-Y. Su, T. Gao, F.-L. Yan, and J.-L. Chen, Phys. Rev. A **98**, 062103 (2018).

[37] R. Rabelo, L. Y. Zhi, and V. Scarani, Phys. Rev. Lett. **109**, 180401 (2012).

[38] A. Acín, R. Gill, and N. Gisin, Phys. Rev. Lett. **95**, 210402 (2005).

[39] N. Brunner, N. Gisin, and V. Scarani, New Journal of Physics **7**, 88–88 (2005).

[40] M. Junge and C. Palazuelos, Communications in Mathematical Physics **306**, 695–746 (2011).

[41] Y.-C. Liang, T. Vértesi, and N. Brunner, Physical Review A **83**, 10.1103/physreva.83.022108 (2011).

[42] T. Vidick and S. Wehner, Physical Review A **83**, 10.1103/physreva.83.052310 (2011).

[43] D. Dilley and E. Chitambar, Phys. Rev. A **97**, 062313 (2018).

[44] W. T. M. Irvine, J. F. Hodelin, C. Simon, and D. Bouwmeester, Phys. Rev. Lett. **95**, 030401 (2005).

[45] J. S. Lundeen and A. M. Steinberg, Phys. Rev. Lett. **102**, 020404 (2009).

[46] K. Yokota, T. Yamamoto, M. Koashi, and N. Imoto, New Journal of Physics **11**, 033011 (2009).

[47] A. Aspect, J. Dalibard, and G. Roger, Phys. Rev. Lett. **49**, 1804 (1982).

[48] Y.-H. Luo, H.-Y. Su, H.-L. Huang, X.-L. Wang, T. Yang, L. Li, N.-L. Liu, J.-L. Chen, C.-Y. Lu, and J.-W. Pan, Science Bulletin **63**, 1611 (2018).

[49] M. Freyberger, Phys. Rev. A **51**, 3347 (1995).

[50] A. S. Majumdar and N. Nayak, Phys. Rev. A **64**, 013821 (2001).

[51] D. N. Matsukevich, P. Maunz, D. L. Moehring, S. Olmschenk, and C. Monroe, Phys. Rev. Lett. **100**, 150404 (2008).

[52] J. Hofmann, M. Krug, N. Ortegel, L. Gérard, M. Weber, W. Rosenfeld, and H. Weinfurter, Science **337**, 72 (2012), <https://www.science.org/doi/10.1126/science.1221856>.

[53] M. Neeley, R. C. Bialczak, M. Lenander, E. Lucero, M. Mariantoni, A. D. O’Connell, D. Sank, H. Wang, M. Weides, J. Wenner, Y. Yin, T. Yamamoto, A. N. Cleland, and J. M. Martinis, Nature **467**, 570 (2010).

[54] L. DiCarlo, M. D. Reed, L. Sun, B. R. Johnson, J. M. Chow, J. M. Gambetta, L. Frunzio, S. M. Girvin, M. H. Devoret, and R. J. Schoelkopf, Nature **467**, 574 (2010).

[55] S. Das and G. Paul, ACM Transactions on Quantum Computing **1**, 1 (2020).

[56] T. Hou, D. Ding, C. Wang, X.-c. Zhang, and Y.-q. He, International Journal of Theoretical Physics **60**, 1972 (2021).

[57] See Supplemental Material at [URL will be inserted by publisher] for [give brief description of material].

[58] Y. Aharonov, A. Botero, S. Popescu, B. Reznik, and J. Tollaksen, Physics Letters A **301**, 130 (2002).

[59] The code in this work can be accessed at: <https://github.com/mx73/Testing-QM-on-NISQ>.

[60] D. M. Tran, D. V. Nguyen, B. H. Le, and H. Q. Nguyen, EPJ Quantum Technology **9**, 6 (2022).